# PIV Measurements of a Double Annular Jet for validation of numerical simulations

**Broeckhoven Tim[1], Brouns Mark[2], Vanherzeele Joris[3], Vanlanduit Steve[4] and Lacor Chris[5]**

1: Department of Mechanical Engineering, Vrije Universiteit Brussel, Brussels, Belgium, tim@stro.vub.ac.be
2: mark@stro.vub.ac.be 3: joris.vanherzeele@vub.ac.be
4: steve.vanlanduit@vub.ac.be 5: chris@stro.vub.ac.be

**Abstract** Although numerical simulation of turbulent flows has made a huge progress over the past decades with simulation techniques like RANS and LES and an exponential increase in available computer power, there is still a high demand for experimental validation data for complex turbulent flows. Turbulence closures often make assumptions that must be validated and contain parameters that have to be tuned, using available databases for different flow configurations. Direct Numerical Simulation data is only available for simple geometries and relatively low Reynolds numbers because of the extremely high computational cost. Detailed measurements of mean velocity fields and turbulent intensities are needed to investigate the capability of turbulence models to adequately represent the complex physics of the flow when phenomena like recirculation, anisotropy and swirl are present.The generation of empirical databases is thus essential, but complete databases are still rare for complex flow configurations. The geometry considered in the investigation is a prototype of a non-premixed industrial double annular burner. Since international norms on the emission of pollutants are getting more and more strict, a better understanding of the flow field, mixing processes and combustion processes in such devices is essential. A correct prediction of the mixing is a key factor to describe the turbulent combustion process correctly. Therefore, in a first step the burner is investigated in cold conditions and the behaviour and interaction of the annular jets is studied. Detailed validation data – average velocity fields, Reynolds stresses, vorticity and turbulent kinetic energy – are presented and the complex physics of the flow are described. The position of several stagnation points and vortex centers that are present in the considered flow field can be used to assess numerical simulations. The obtained PIV results are compared with results from a former LDA investigation in order to assess the quality and reliability of the measurements in different regions of the flow.

## 1. Introduction

Industrial devices in fluid engineering quite often involve complex turbulent flows. This is the case for example in the combustion chamber of turbine engines, in industrial furnaces and in other burners. A better understanding of the flow field, mixing processes and combustion processes in such industrial devices is challenging in the context of energy savings and environmental concerns linked to pollution and global warming. A correct prediction of the mixing is a key factor to describe the turbulent combustion process correctly. Therefore, in a first step burners can be investigated in cold conditions studying the complex physics of the flow with phenomena like mixing, recirculation, anisotropy and swirl. Many turbulence models used in numerical simulations fail to predict the correct flow behaviour in such complex flows. Several assumptions are made that must be validated and the models contain parameters that have to be tuned, using available databases for different flow configurations. Thus there is still a need for detailed empirical databases for these type of flow configurations. The paper is structured as follows. In section 2 the considered burner configuration and the experimental setup are described. In section 3 the used measurement and postprocessing methods of the data are discussed. Detailed validation data –

average velocity fields, Reynolds stresses, vorticity and turbulent kinetic energy – are presented in section 4 and the complex physics of the flow are described. In order to assess the quality and reliability of the measurements in different regions of the flow the obtained PIV results are compared with results from a former LDA investigation in section 5. Finally a conclusion section will close the paper.

## 2. Setup

The geometry considered in the investigation is a prototype (scale 2:1) of a 100kW non-premixed industrial double annular burner with a central pipe supplying the fuel and two coaxial annular orifices supplying the air. Since a correct prediction of the mixing is a key factor to describe the turbulent combustion process correctly, in a first step the burner is investigated in cold conditions and the behaviour and interaction of the annular jets is studied. The central fuel jet having a very low velocity has therefore been neglected. Figure 1 shows the considered burner with the major dimensions.

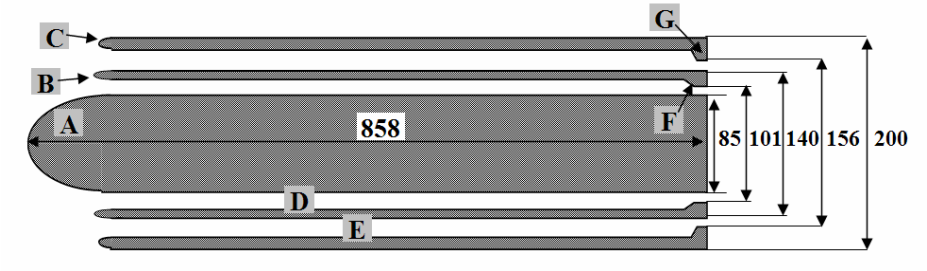


**Figure 1 Double annular burner geometry with major dimensions in mm**

The entry to the burner is made smooth with bullets of ellipsoidal shape (A,B & C) to avoid separation. Two ducts (D & E) of respectively 16.3 mm and 18.2 mm produce the primary and secondary flows. At the exit of the nozzle, two annular pieces act as contracting nozzles (F & G) and reduce the exit area to increase the velocity without pressure losses. The smooth shape of the contraction is created by merging two quarter-circles but can cause some separation for high flow rates. At the nozzle exit both annular channels have a width of 8mm and because of the chosen geometry and contraction ratios have almost the same bulk velocity. The inlet and outlet section of the burner are shown in figure 2.

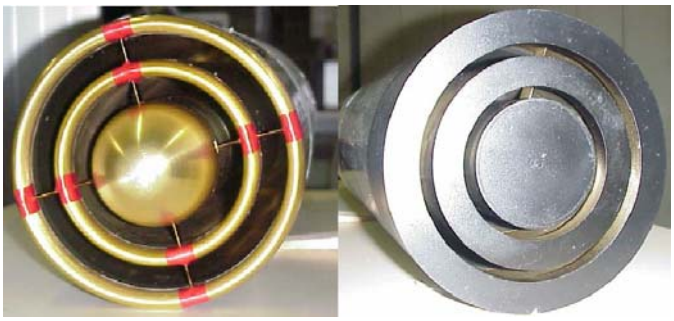

**Figure 2 Inlet and outlet of the burner**

Figure 3 shows the overall experimental setup. A compressor whose rotation speed is precisely measured by an incremental shaft encoder, provides the air which flows through an inlet arrangement, the actual burner and into the combustion chamber. A tube brings the air from the compressor into the settling chamber and through two wire mesh screens, with 0.3 mm diameter

wires in square grids of size 1.67 mm, placed 100 mm apart. The air enters a conical diffuser (14˚ cone angle) towards the plenum chamber where the burner is inserted. Several supports are used to ensure a precise alignment of the axis of the burner and the plenum chamber. This arrangement proposed in Hazarika and Hirsch (1998) was devised in order to obtain good axisymmetric conditions at the entrance of the burner. The cold combustion chamber positioned at the end of the burner has an inner diameter of 382 mm and a length of 1180 mm. In order to allow optical access a transparent window with axial length of 285 mm and vertical aperture of 350 mm was installed just downstream the burner exit. At the exit of the chamber a glass plate, with four circular holes to evacuate the flow, allows optical access. Former investigations Schmitt et al. (2000), Hazarika et al. (2001), Schmitt and Hirsch (2001), Frania and Hirsch (2004) and Frania et al. (2005) have used this experimental setup for 2D and 3D LDA measurements, to analyze vortex unsteadiness and turbulence and to assess the nonlinear constitutive equation (Boussinesq hypothesis).

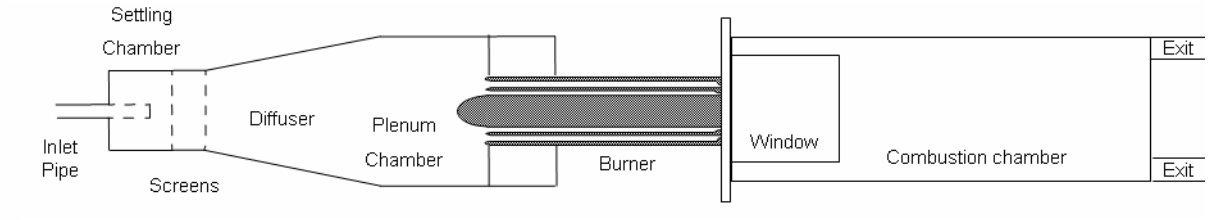


**Figure 3 Complete experimental configuration**

**Table 1 Main geometrical and flow parameters for the considered double annular jet**

| Parameter | Description | Dimension |
|---|---|---|
| $r_1$ | Outer radius primary jet | 50.5 mm |
| $r_2$ | Outer radius secondary jet | 78.0 mm |
| dr | Width annular jets | 8.0 mm |
| $r_c$ | Radius combustion chamber | 191.0 mm |
| $U_1$ | Bulk-averaged velocity primary jet | 6.3 m/s |
| $U_2$ | Bulk-averaged velocity secondary jet | 6.2 m/s |
| $\beta = \frac{r_2}{r_1}$ | Secondary to primary radius ratio | 1.55 |
| $\alpha = \frac{U_2}{U_1}$ | Secondary to primary velocity ratio | 0.98 |

Table 1 shows the main geometrical and flow parameters of the configuration. The Reynolds number based on the outer diameter of the secondary jet and its bulk velocity is about 60,000.

The vertical laser sheet is generated with a New Wave Minilase II Nd-Yag laser (532 nm wavelength, 100mJ/pulse) positioned behind the combustion chamber on the centerline. The seeding particles used are 1μm DEHS oil droplets introduced at the beginning of the diffuser. A 5Hz PCO sensicam QE camera is used to record the images in a vertical plane through the center of the combustion chamber.

## 3. Method

To obtain accurate validation data, the region of interest reaching about 200 mm in axial direction, has been split in 5 measurement areas as can be seen in Figure 4. Due to the limitation of the optical access window the field of view starts 2mm behind the nozzle exit. In each of the sections 5000 image pairs were recorded. The pulse delay of 80 µs was determined so that a particle displacement of approximately 3 pixels between two consecutive images was obtained in the regions of high velocities. The images were analyzed using the PIVview 1.7 software package (PIVTEC GmbH, Göttingen Germany). A cross-correlation FFT with adaptive multi-pass procedure was used to generate the vector fields. A double (Hart) correlation was applied to increase detectability of the correlation peak associated with the particle shift. An interrogation window of 32x32 pixels on each pass with an overlap of 50% was used. After the first pass, the vector field was filtered for outliers using a maximum pixel displacement difference of 3 pixels. Less than 1% of the vectors had to be interpolated. A least squares 3-point Gauss fit algorithm was used to recover the sub-pixel displacement of the correlation. An in-house software was used to average the measured 2D velocity fields and to merge the measurement areas by interpolating the obtained data in the overlapping regions.

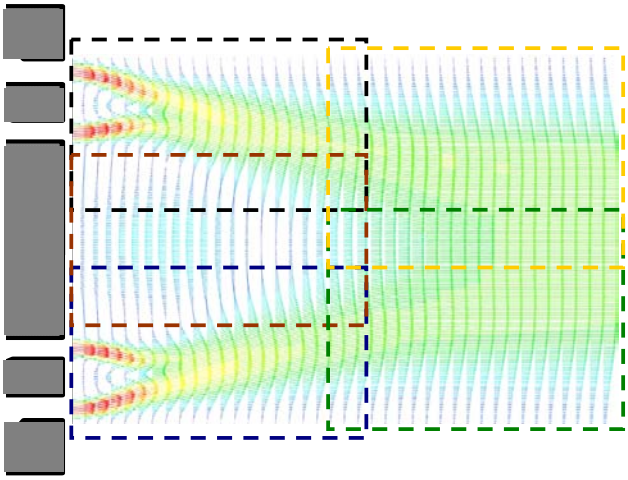

**Figure 4 Different measurement areas in the zone of interest**

The instantaneous velocity in streamwise (x) direction is u and the instantaneous velocity in radial (y) direction is v. Turbulence intensities and Reynolds stresses were calculated according to:

$$\begin{aligned} \langle u'u' \rangle &= \langle u^2 \rangle - U^2 \\ \langle v'v' \rangle &= \langle v^2 \rangle - V^2 \\ \langle u'v' \rangle &= \langle uv \rangle - UV \end{aligned} \tag{1}$$

with $U = \langle u \rangle$ and $V = \langle v \rangle$ the time averaged velocity fields and $u'$ and $v'$ the fluctuating velocity components. The kinetic energy of the in plane components can then be calculated as

$$k = \frac{1}{2}\left( \langle u'u' \rangle + \langle v'v' \rangle \right) \tag{2}$$

The vorticity and shear components were calculated as

$$\omega_z = \frac{\partial U}{\partial y} - \frac{\partial V}{\partial x}$$
$$S_{xx} = \frac{\partial U}{\partial x} \quad S_{yy} = \frac{\partial V}{\partial y} \quad S_{xy} = \frac{1}{2}\left(\frac{\partial U}{\partial y} + \frac{\partial V}{\partial x}\right) \tag{3}$$

## 4. Results

Figure 5 shows the averaged velocity magnitude field together with the average streamline pattern and it can be seen that the flow is almost fully axi-symmetric. Several different zones can clearly be distinguished. The zoomed area shows the two annular jets first join, to form a single annular jet about 20mm behind the nozzle exit, and in between a set of annular counter-rotating vortices is created. The outer annular jet bends a little towards the centreline of the burner while the inner jet bends away from the centreline. The stagnation point where the two annular jets merge is located a few mm below the middle of the annular nozzle exists showing that the total flow is bending slightly towards the centreline. Then the single annular jet develops towards a central jet about 75mm behind the nozzle exit, creating a big central toroidal vortex. One can also observe that an elongated recirculation zone occurs outside the outer annular jet caused by the entrainment and the confined combustion chamber. In Figure 6 the non-dimensional ($U_o$=6.3m/s) streamwise and radial velocity components are shown. The big central recirculation zone and small recirculation zones between the annular jets with negative streamwise velocity can be clearly observed. At the top the negative radial velocity in the outer annular jet and positive radial velocity in the inner annular jet show both jets merge and then a negative radial velocity indicates the transition of a single annular jet towards a central jet.

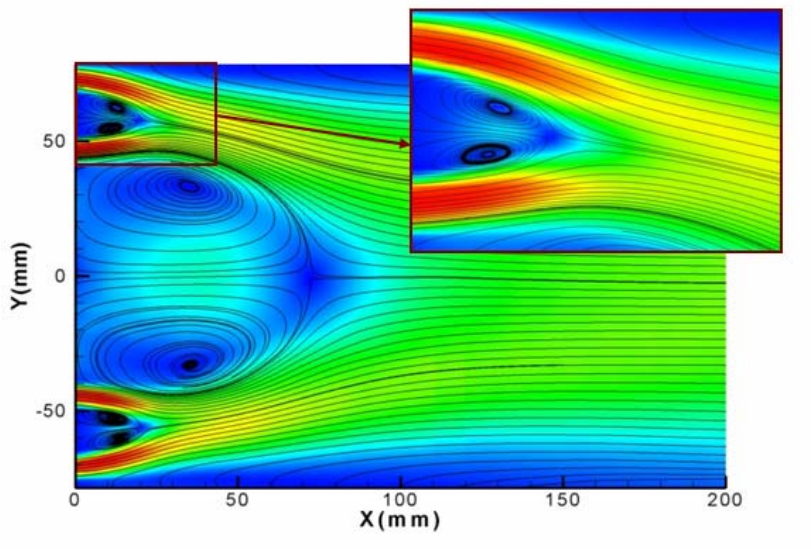


**Figure 5 Averaged Velocity Magnitude (Colour Contours) and streamlines**

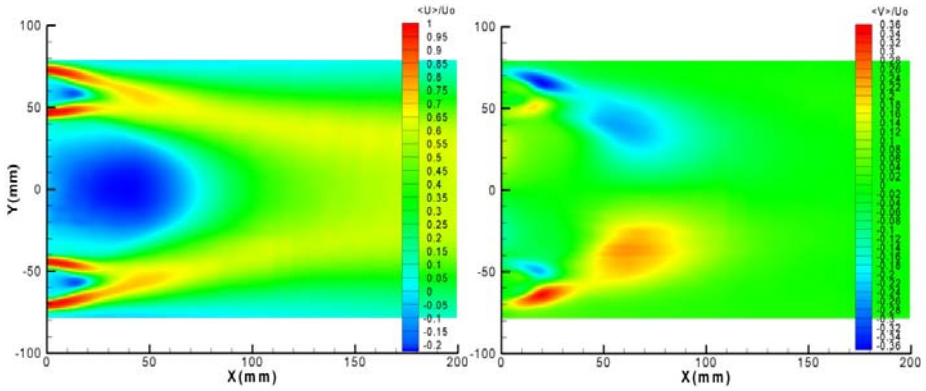


**Figure 6 Average normalized streamwise and radial velocity**

The normalized second moments – turbulent intensities, Reynolds stress and kinetic energy – are shown in Figure 7. The streamwise velocity fluctuations $\langle u'u' \rangle$ are high in the shear layers of the two annular jets, further downstream in the outer shear layer of the single annular jet and the outer shear layer of the central jet and in the shear layer between the single annular jet and the central toroidal vortex. The radial turbulent intensity $\langle v'v' \rangle$ is the highest around the stagnation point where the two annular jets merge and around the central stagnation point where the single annular jet develops into a single jet. The Reynolds stress component $\langle u'v' \rangle$ is high in the shear layer between the two annular jets and the annular counter-rotating vortices and between the single annular jet and the central toroidal vortex. The kinetic energy field of the in-plain components shows that several zones of intense mixing are present in the flow.

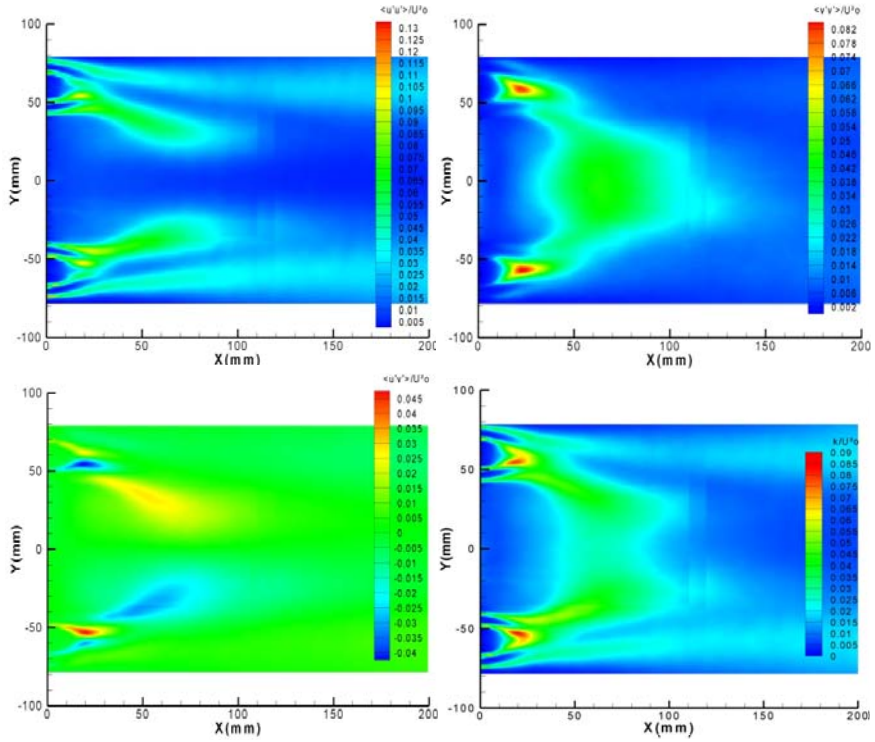


**Figure 7 Reynolds stress components and turbulent kinetic energy**

Figure 8 shows the normalized turbulent intensities $\langle u'u' \rangle$ and $\langle v'v' \rangle$, the Reynolds stress $\langle u'v' \rangle$ and the kinetic energy in four radial sections. One can clearly see the different zones described before. At the inlet only the axial fluctuations contribute to the kinetic energy and are big in the shear layers of the two annular jets because of the high velocity gradients shown in Figure 9. The second radial cut is located just before the two annular jets merge with a high radial turbulent intensity and high Reynolds stress off opposite sign in the two contra rotating vortices between the jets. In the third cut the two peaks in axial turbulence correspond to the inner and outer shear layer of the single annular jet and in the centre the higher radial turbulent intensity corresponds to the central toroidal vortex. One outer jet diameter behind the burner, the flow has developed towards a single jet with highest kinetic energy in the shear layer of this jet.

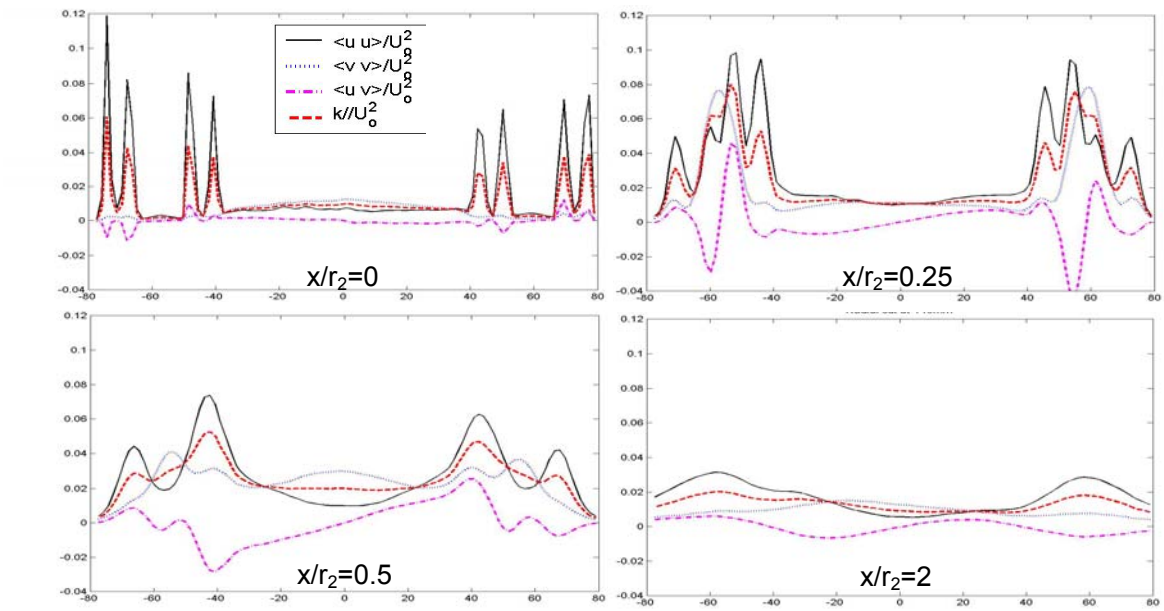


**Figure 8 Normalized turbulent intensities, Reynoldsstress and kinetic energy**

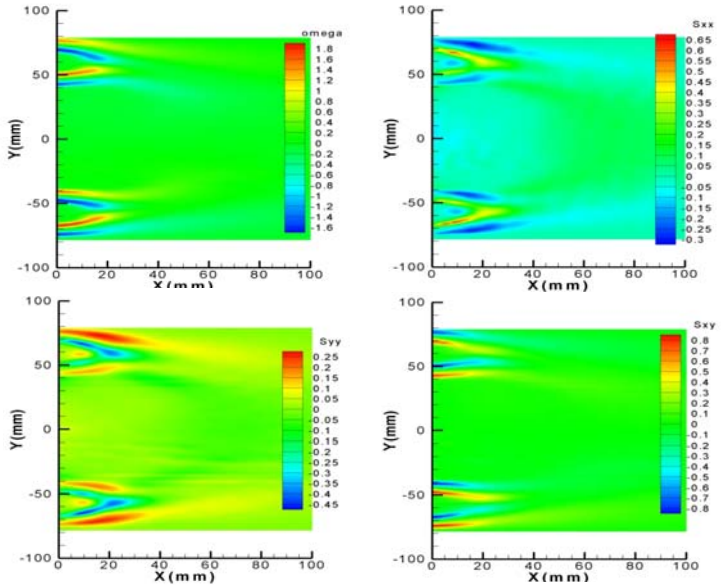


**Figure 9 Vorticity and strain components**

When looking at the flow field in Figure 8 one can distinguish several points that can be used as assessment points for comparison with numerical simulations and for validation of turbulence models. Point A is the central stagnation point, $B_1$ and $B_2$ are lying on a circular line in the center of the central toroidal vortex, $C_1$ and $C_2$ correspond to the stagnation line where the two annular jets merge. The stagnation points are characterized by a zero mean axial and radial velocity but high kinetic energy and radial velocity fluctuations. The centers of the smaller vortices between the two jets are given by $D_1$,$D_2$ and $E_1$,$E_2$. Table 2 gives the position of the different points made dimensionless with the outer radius of the outer jet $r_2$ =0.078 m.

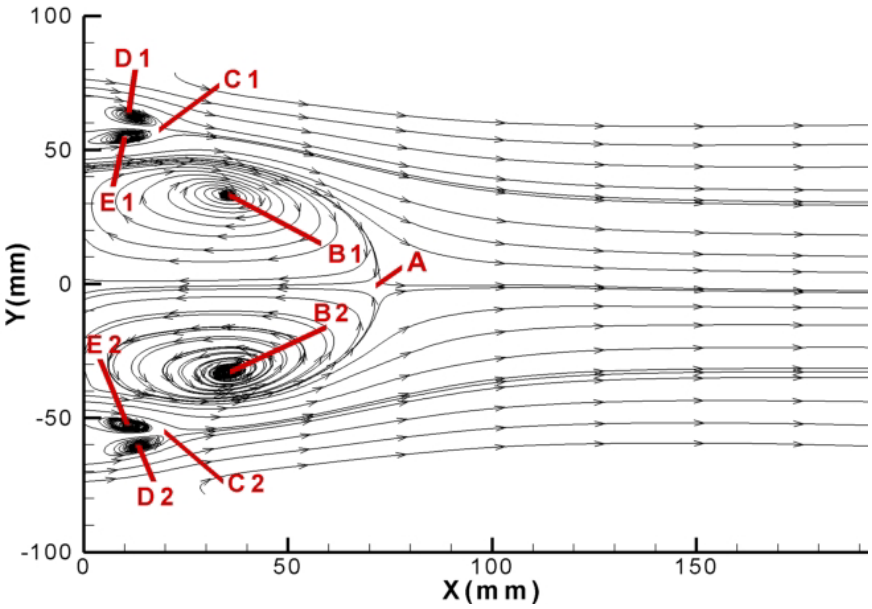


**Table 2**

**Position assesment points**

| Point | $(x/r_2,y/r_2)$ |
|---|---|
| A | (0.95,-0.01) |
| $B_1$ | (0.48, 0.43) |
| $B_2$ | (0.48,-0.42) |
| $C_1$ | (0.27, 0.74) |
| $C_2$ | (0.28,-0.72) |
| $D_1$ | (0.18, 0.80) |
| $D_2$ | (0.19,-0.77) |
| $E_1$ | (0.16, 0.70) |
| $E_2$ | (0.17,-0.68) |

**Figure 10 Stagnation points and vortex centers used as assessment parameters**

From the table it can be seen that the alignment of the setup is good and that the velocity of the annular jets at nozzle exits is nearly axisymmetric resulting in an almost axisymmetric flow field. 3D LDA measurements Frania et al. (2005) have shown that the average tangential velocity is small, in other words there is no significant swirl. Of coarse this does not mean that there is no instantaneous velocity in tangential direction. In the measurements of Frania et al. (2005) tangential turbulent intensities up to 50% of the axial turbulent intensity have been measured near the stagnation points $C_1$ and $C_2$. Also recent LES simulations by the present authors have shown that three dimensional vortical structures are present in the flow. An instantaneous snapshot of the top part of the flow field in Figure 11 shows the turbulent nature of the flow and the presence of vortical structures of different size and intensity.

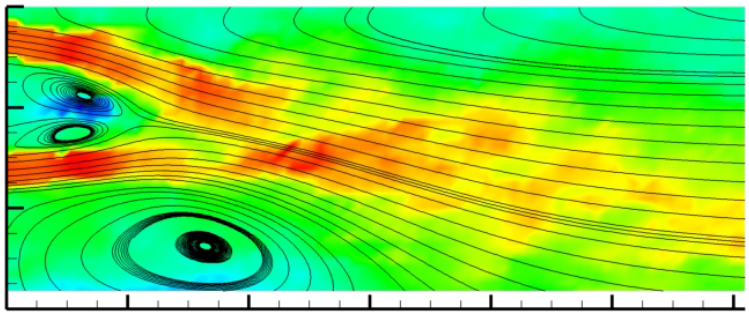

**Figure 11 Instantaneous velocity field superimposed with mean streamlines**

A complete database with averaged axial and radial velocity (U,V), turbulent intensities (<u'u'>, <v'v'>) and Reynolds stress (<u'v'>) has been generated. The data is available in a domain of 200mm in axial direction and 80mm in radial direction on a grid of 1.5x1.5 mm and will be made accessible through the web to be used as validation data for numerical simulations. Recently several RANS models have been tested on the considered configuration Geerts et al. (2005), QNET-CFD, and both mean fields of velocity and turbulent kinetic energy as well as the assessment points have been used to compare the ability of the turbulence models to predicted the complex physics present in the flow.

## 5. Comparison with LDA

In order to assess the quality and reliability of the measurements in the different regions of the flow the PIV measurements are compared with the LDA data of Schmitt et al. 2000, Schmitt et al. 2001 and Frania et. al. 2005. To make a quantitative comparison the data in terms of mean axial and radial velocities in several radial cuts are compared in Figure 12 and along the centreline of the combustion chamber in Figure 13 where also the Reynolds stress components and kinetic energy are compared.

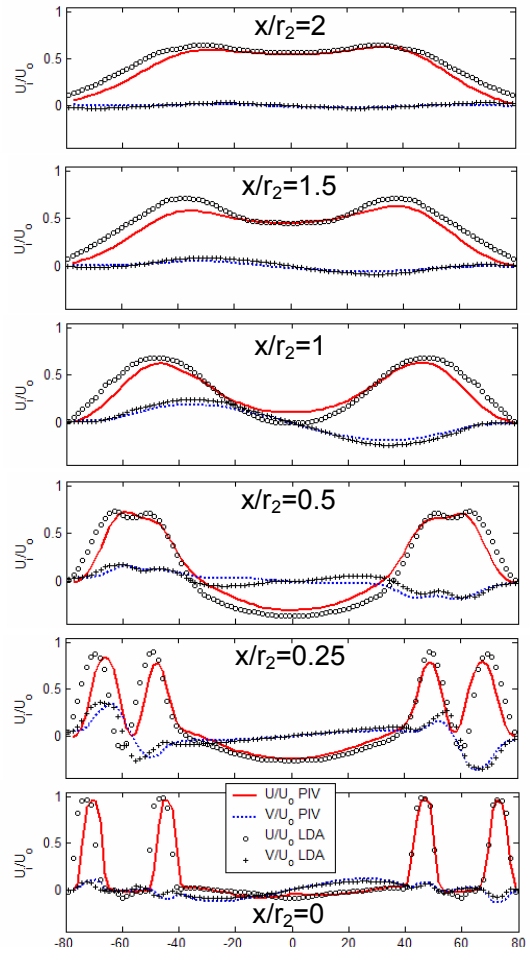


**Figure 12 Comparison of PIV and LDA: mean axial and radial velocity in radial cuts**

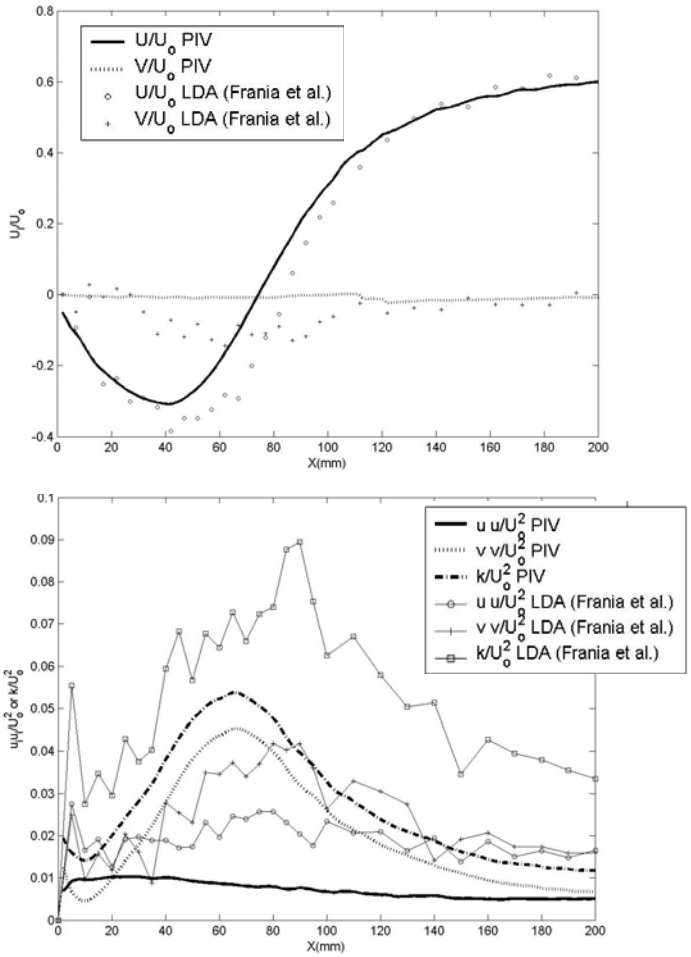


**Figure 13 Mean velocities, Reynolds stress components and kinetic energy along centerline**

Frania et al. (2005) performed 3-component LDA measurements on a rather coarse measurement grid along 36 vertical sections, ranging from $X/r_2 = 0$ to $X/r_2 = 3.2$, distributed non-uniformly to have several traverses in each zone of the flow (two annular jets, single annular jet, single central jet). The measurement nodes were unevenly distributed along the traverses: in calm zones, the space between consecutive measurements was 2 to 4 mm, whereas for more turbulent zones, this distance was 0.5 mm. In total the measurements have been performed for 5500 different node positions and for each position several thousand particles (dry stick incense smoke) have been recorded. This raw data has been linearly interpolated on a finer and regular grid and was symmetrized (i.e. for a given value of X the values at position (X,Y) and (X,-Y) are averaged). In Figure 12 this smoothed data has been used for comparison while in Figure 13 the raw data in the 36 measurements points on the centreline of the combustion chamber have been used for comparison. It can be seen that the non-uniform measurement grid is rather coarse and that some unphysical variations are present in the measured values. These might be caused by the fact that measurements have been made over a period of several weeks leading to possible small changes in setup geometry, variations in the air feeding system and a deposition of smoke particles (Frania et al. private communication).

In Figure 12 it can be seen that the PIV (full lines) and LDA (symbols) measurements of mean velocities are in good agreement. Further downstream the nozzle exit the axial velocity profiles show that the single jet predicted in the LDA measurements is a bit wider. Comparing the streamline pattern of both measurements (not shown here) one can notice that the single central jet in the LDA measurements seems to start spreading earlier while in the PIV measurements it keeps a constant radius till the end of the measurement domain. It must also be noted that the LDA measurement grid is rather coarse in this zone. In the mean velocity plot of Figure 13 one can see that the length of the mean recirculation zone measured by the LDA is a bit longer. This difference might be caused by small differences in the mean bulk velocity of the inner and outer jet. It is known that the position of the stagnation point is sensitive to the ratio $U_2/U_1$ (see table 1) which was about 1% lower in the measurements of Frania et al (2005). Another reason might be the difference in inertia of the used seeding particles - 1µm DEHS oil droplets for the PIV and dry stick incense smoke for the LDA. It can also be seen that the PIV measurements predict a more realistic behaviour of the mean radial velocity on the centreline which should be zero in a perfectly axisymmetric flow. The radial turbulent intensity on the centreline determined from the LDA and PIV data is of similar magnitude but the maximum value is located further downstream in the LDA measurements, which is in agreement with the bigger recirculation zone. The axial turbulent fluctuation level on the centreline measured by the LDA is about twice bigger than by PIV. Possibly fluctuations of high frequency are present in the flow which can not be measured because of the limitation of the 5Hz PIV camera resulting in a lower level of measured turbulent intensities. Moreover in the 3D LDA measurements also the tangential turbulent intensity is available resulting in a higher kinetic energy as can be seen from Figure 13.

## 6. Conclusions

In this paper a PIV-investigation of a prototype industrial double annular burner has been performed. Detailed validation data - mean velocities, Reynolds stress components and turbulent kinetic energy - have been presented. The structure of the complex flow was qualitatively described with contour plots of different quantities in the entire flow field and the position of several points that can be used as assessment points for comparison with numerical simulations has been discussed. In order to assess the quality and reliability of the measurements in the different regions of the flow the PIV measurements are compared with the LDA data of Frania et. al. 2005.

## 7. Acknowlegdements

The authors gratefully acknowledge the financial support by the Flemish Research Foundation (FWO-Flanders) under project G.0130.02 and thank T. Frania for making the LDA data available for comparison.

## 8. References

Frania T., Hirsch Ch., " Measurements of the Turbulent Flow Field generated by a Single Annular Jet", XVI National Conference on Fluid Mechanics, Waplewo, Poland, 2004

Frania T., Geerts S., Hirsch Ch., " Measurement of the 3D Turbulent Flow Field of a Confined Double Annular Jet", AIAA paper No. 2005-5154, AAIA 4th Theoretical Fluid Mechanical Conference, 6-9 June, Toronto, Ontario, 2005

Geerts S., Hirsch Ch., Broeckhoven. T., Lacor Ch., " Validation of CFD and Turbulence Models for Confined Double Annular Jet", AIAA paper No. 2005-5317, AAIA 4th Theoretical Fluid Mechanical Conference, 6-9 June 2005, Toronto, Ontario", 2005

Hazarika B. K. and Hirsch Ch., "The flow field in the nozzle region of a confined double annular jet", F. W. O. (Flemish Research Foundation) Project Contract Report, Report Nº STR-TN-3/98, Vakgroep Stromingsmechanica, VUB, Brussels, 52 pp, 1998

Hazarika B. K., Vucinic D., Schmitt F., Hirsch Ch., "Analysis of toroidal vortex unsteadiness and turbulence in a confined double annular jet", 39th Aerospace Sciences Meeting&Exhibit, AIAA paper 2001-0146, Reno, USA, 2001

Schmitt F. and Hirsch Ch., "Direct experimental assessment of the nonlinear constitutive equation for a complex flow", 39th Aerospace Sciences Meeting&Exhibit, AIAA paper 2001-0881, Reno, USA, 2001.

Schmitt F. and Hirsch Ch., "Direct test of Boussinesq's hypothesis and the K-transport equation using experimental, DNS and LES data, in Engineering Turbulence Modelling and Experiments", 5 édité par W. Rodi and N. Fuyeo, Elsevier, 2002, pp. 167-176.

Schmitt F., Hirsch Ch., Hazarika B.K., "LDA measurements in the nozzle region of a confined double annular burner: statistical analysis and model evaluation", Lisboa 2000: 10th International Symposium on Applications of Laser Techniques to Fluid Mechanics, Lisbon, Portugal, 2000, 16pp.

Schmitt F., Hazarika B.K., Ch. Hirsch, "LDV measurements of the flow field in the nozzle region of a confined annular burner," Trans. ASME, Journal of Fluid Engineering, 123, 2, 228-236, 2001.

QNET CFD, Thematic Network on Quality and Trust for the industrial applications of Computational Fluid Dynamics, Application Challenge 7, Confined Double Annular Jet, http://www.qnet-cfd.net